Chinese Chemical Letters 35 (2024) 108957

Contents lists available at ScienceDirect

Chinese Chemical Letters

journal homepage: www.elsevier.com/locate/cclet

Zero thermal expansion in $Cs_2W_3O_{10}$

Juan Guo, Mingyuan Fang, Qingsong Liu, Xiao Ren, Yongqiang Qiao, Mingju Chao, Erjun Liang, Qilong Gao*

School of Physics & Microelectronics, Key Laboratory of Materials Physics of Ministry of Education of China, Zhengzhou University, Zhengzhou 450052, China

ARTICLE INFO

Article history:
Received 20 June 2023
Revised 22 July 2023
Accepted 21 August 2023
Available online 23 August 2023

Keywords:
Zero thermal expansion
Cesium tungstate
Raman spectra
Average atomic volume
Temperature-dependent X-ray diffraction

ABSTRACT

Zero thermal expansion materials are important for the practical applications due to their shape stability as changing temperature. The reported concept of average atomic volume is an available method to hunt new zero thermal expansion materials. Here, according to this concept, a tetragonal tungstate $Cs_2W_3O_{10}$ with zero expansion has been found. There is no structure phase transition as increasing temperature from 150 K to 573 K. The coefficient of thermal expansion of axes and volume are $\alpha_a = 0.0074 \times 10^{-6}$ K^{-1}, $\alpha_c = 1.63 \times 10^{-6}$ K^{-1}, and $\alpha_V = 1.60 \times 10^{-6}$ K^{-1}, respectively, in the temperature range of 150 ~ 573 K. The temperature- and pressure-dependent Raman spectra reveal that the vibrations of WO_6 octahedra libration modes with positive total anharmonicity and W-O-W bending mode with negative Grüneisen parameter are possibly the origin of zero thermal expansion in $Cs_2W_3O_{10}$.

It is well known that the phenomenon of thermal expansion and cold contraction exists in most materials. The coefficient of thermal expansion (CTE) is a parameter used to characterize the expansion properties of solid materials. The mismatch of CTE is an issue in fields of electric devices [1], solid oxide fuel cells [2], thermoelectric materials [3], *etc.*, which seriously restricts the applications of functional materials. Many efforts have been performed to solve the mismatch of CTE, of which exploring materials with zero thermal expansion (ZTE) is a feasible way. Due to the great advantage of adjusting thermal expansion, the study of negative thermal expansion (NTE) received great attention [4–12]. One way is that preparation of composite materials with NTE and PTE materials such as ZrW_2O_8/Al [13], ZrW_2O_8/ZrO_2 [14], ScF_3/Cu [15] and $Zr_2WP_2O_{12}$/PI [16]. Another way is that use chemical modification (element substitution or guest insertion) in NTE compounds to achieve ZTE behavior such as $(Zr,Sn)Mo_2O_8$ [17], $(Ta,Ti)(Mo,V)O_5$ [18], $Hf_{0.85}Ta_{0.15}Fe_2C_{0.01}$ [19], $Na_xFeFe(CN)_6$ [20], mesopores $PbTiO_3$ [21], and $TiCo(CN)_6{\cdot}2H_2O$ [22]. There are also some inherent ZTE compounds such as $FeCo(CN)_6$ [23], $Ta_2Mo_2O_{11}$ [24], $Zn_4B_6O_{13}$ [25] and $ZrMgMo_3O_{12}$ [26]. It should be noted that the ZTE compounds are very few. Recently, a new concept of "average atomic volume (AAV)" has been proposed by Gao *et al.* [27,28], which can be used to explore potential zero or negative thermal expansion in the open-framework materials. According to the concept, the value of AAV can be calculated by the equation $AAV = V/(Z \times N)$ where V is unit cell volume, Z is cell formula units, and N is the number of atoms in the chemical formula. As the value of AAV is ~16 Å^3, the ZTE occurs.

Inspired by the concept of AAV, we investigated some tungstates because most of them belong to open-framework materials. Fortunately, a kind of cesium tungstate $Cs_2W_3O_{10}$ reported firstly in 1996 [29] has been found. Based on the structure data of $Cs_2W_3O_{10}$, we can find that the V is 2636.89 Å^3, Z is 11 and N is 15, so its AAV is 15.98 Å^3. Due to its AAV is exactly equal to 16 Å^3, which means that it can be as a probable candidate for ZTE materials. Tetragonal $Cs_2W_3O_{10}$ with space group $I\bar{4}$ possesses a framework structure formed by corner-sharing WO_6 octahedra together with Cs atoms residing in the WO_6 framework. It is one of important functional materials and has been researched in the fields of optics and catalysis [30–32]. However, the thermal expansion properties of $Cs_2W_3O_{10}$ have not been studied to the best of our knowledge.

In this work, the crystal structure and thermal expansion of $Cs_2W_3O_{10}$ were investigated by temperature-dependent X-ray diffraction (XRD). The ZTE appeared along both *a*- and *c*- axis, and also in volume. Especially, the CTE of *a*-axis is very small, which should be caused by the chains of WO_6 octahedra in *ab*-plane. The mechanism of ZTE also is discussed based on the results of temperature- and pressure-dependent Raman spectra. The librations of WO_6 octahedra and W-O-W bendings should be related to the ZTE.

In order to determine the purity of sample, the XRD data have been collected at room temperature, of which Rietveld refinement

* Corresponding author.
E-mail address: qilonggao@zzu.edu.cn (Q. Gao).

https://doi.org/10.1016/j.cclet.2023.108957
1001-8417/

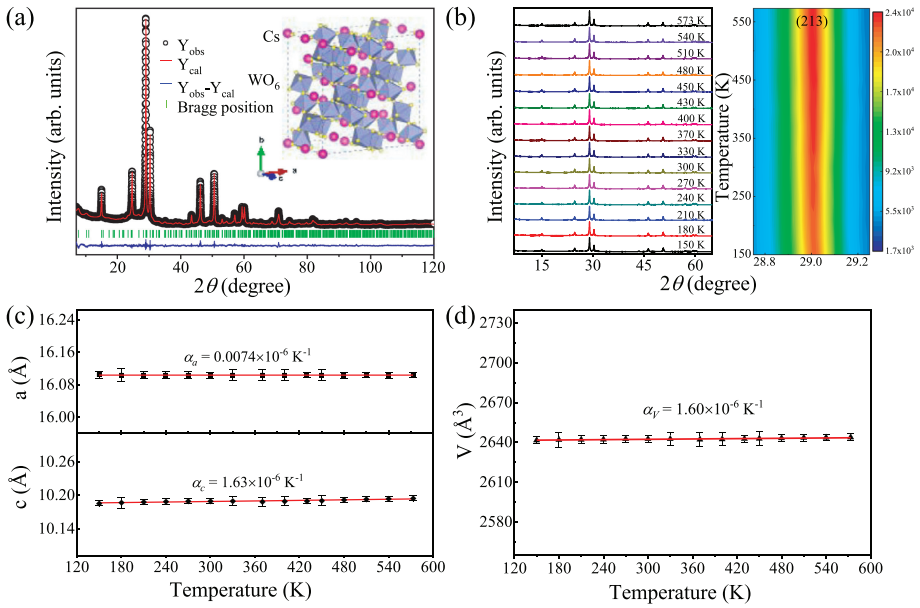

Fig. 1. (a) Rietveld refinement patterns at room temperature. (b) XRD patterns at different temperature and temperature dependence of cell parameters. (c) *a*, *c* and (d) *V* and of $Cs_2W_3O_{10}$. The inset is the schematic diagram of $Cs_2W_3O_{10}$.

also has been performed. The observed, calculated and difference patterns are displayed in Fig. 1a. The reliability factors (R_{wp}, R_p, R_R) listed in Table S1 (Supporting information) are less than 10%, indicating that the refinement result is satisfactory. The cell parameters, space group, atom position, occupancy, isotropic atomic displacement parameters (*B*) are also listed in Table S1, which are agreement with those reported in Ref. [29]. It can be seen that tetragonal $Cs_2W_3O_{10}$ with *a*=16.1040(7) Å and *c*=10.1899(4) Å has been obtained. The crystal structure schematic based on the atom positions of sample is shown in the inset of Fig. 1a. The corner-sharing WO_6 octahedra form the framework structure, of which Cs atoms reside in interstices.

To investigate the thermal expansion properties of sample, the temperature-dependent XRD has been performed and XRD patterns at different temperature are displayed in Fig. 1b. It can be seen that the structure phase transition has not been observed as changing temperature from 150 K to 573 K. The cell parameters at different temperature were obtained by Rietveld refinements of XRD data. The temperature dependences of *a*, *c* and *V* have been plotted in Figs. 1c and d. The CTEs obtained by linearly fitting of *a*-*T*, *c*-*T* and *V*-*T* curves are $\alpha_a = 0.0074 \times 10^{-6}\ K^{-1}$, $\alpha_c = 1.63 \times 10^{-6}\ K^{-1}$, and $\alpha_V = 1.60 \times 10^{-6}\ K^{-1}$, respectively. It is clear that ZTE occurs in $Cs_2W_3O_{10}$. The *ab* plane has ultralow thermal expansion and the volume thermal expansion comes from the contribution of *c*-axis. This area ZTE also has been observed in some complex system such as $(C_3H_5N_2)_2K[M(CN)_6]$ [33], $(PPh_4)[Cu_2(CN)_3]$ [34], $[Sr(DMPhH_2IDC)_2]_n$ [35] materials, while very few in oxides. For the volume thermal expansion, it should be noted that $Cs_2W_3O_{10}$ also could be called as ZTE materials because its linear CTE $\alpha_l = \frac{1}{3}\alpha_V$ ($0.53 \times 10^{-6}\ K^{-1}$) is less than $1.0 \times 10^{-6}\ K^{-1}$ according to the description by Sleight [36]. Compared with other ZTE compounds such as $Zn_4B_6O_{13}$ [25], $Mn_3(Cu_{0.55}Sn_{0.45})N$ [37] and $Mg_{1.8}Cu_{0.2}P_2O_7$ [38], $Cs_2W_3O_{10}$ has a quite wide ZTE temperature range.

It is important to clarify the mechanism of abnormal thermal expansion in $Cs_2W_3O_{10}$. In order to achieve that, the Raman spectra have been recorded at different temperature and pressure, respectively. In Fig. 2a, the temperature-dependent Raman spectra have been plotted in the range of 10–1100 cm^{-1}. With raising temperature from 113 K to 673 K, the increase or decrease of Raman peak has not been observed. There is no phase transition during the temperature range, which is in agreement with the results of temperature-dependent XRD. To find the relationship between each vibration mode and temperature, Raman peaks were carefully fitted by Lorentz peak profiles. The temperature-dependent shift of each mode is displayed in Figs. 2c and d. The frequencies of all observed modes exhibit linear dependence on temperature. The slope $d\omega_i/dT$ can be obtained from each ω-*T* curve. The mode description and mode ω_i at ambient temperature and pressure are summarized in Table S2 (Supporting information). The Raman mode description of sample is achieved according to the previous Raman spectroscopic studies on WO_3 and tungstates [39–44]. It can be seen that the 12 vibration modes are observed from 10 cm^{-1} to 1100 cm^{-1}, among which there are 2 modes for WO_6 octahedra libration in ultralow wavenumber, 3 modes for W-O-W bending in low wavenumber, 2 modes for O-W-O bending in middle wavenumber and 5 modes for W-O stretching in high wavenumber. The slopes of the 2 modes for WO6 octahedra libration are positive, while those of other 10 modes are negative as listed in Table S2. Fig. 2b has also shown that the peaks identified as WO_6 octahedra libration below 50 cm^{-1} gradually shift to high wavenumber as increasing temperature. The total anharmonicity of Raman vibration modes has important effects on the thermal expansion of materials [45–48]. According to the formula $\frac{1}{\omega_i}\left(\frac{d\omega_i}{dT}\right)_p$, the total anharmonicity has been calculated and listed in Table S2. Usually, the modes with positive total anharmonicity have contributions to NTE [45–48]. For $Cs_2W_3O_{10}$, it can be seen that 2 modes for WO_6 octahedra libration possess positive total anharmonicity, which should be the origin of abnormal thermal expansion shown in Fig. 1.

The pressure-dependent Raman spectra have been recorded in the range of 10–1100 cm^{-1}. Due to the influence of noise, the Raman peaks below 100 cm^{-1} have not been observed during the measurements. As shown in Fig. 3a, with increasing pressure from atmospheric pressure to 9.00 GPa, the number of vibration modes does not change, which indicates that there is no phase transition under pressure. All peaks corresponding to the Raman modes except 172 cm^{-1} shift to high wavenumber as increasing pressure. Fig. 3b shows the partial magnification of Raman spectra

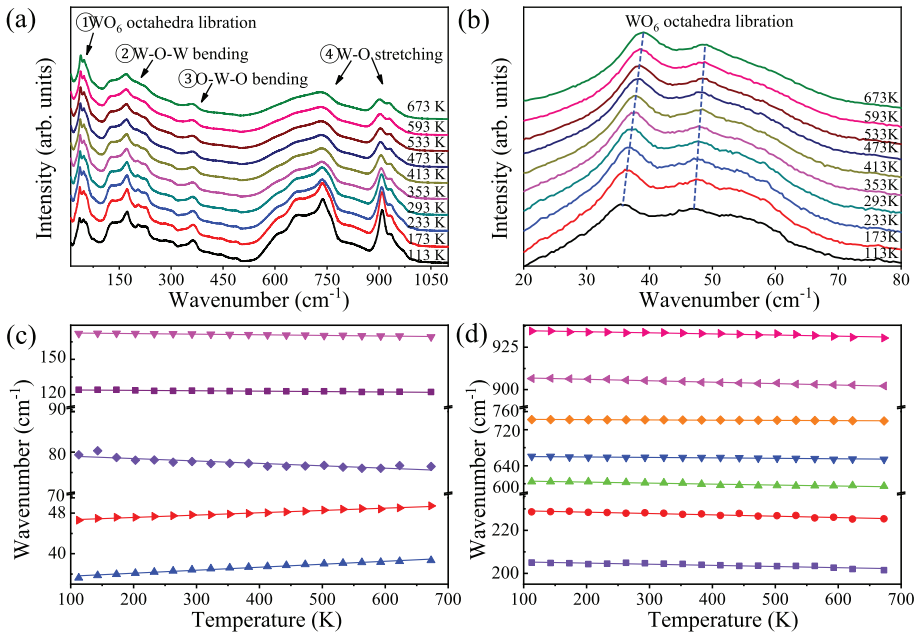

Fig. 2. (a, b) Raman spectra at different temperature and (c, d) temperature dependence of Raman modes of $Cs_2W_3O_{10}$. The solid lines are linear fitting to data of Raman modes at different temperature.

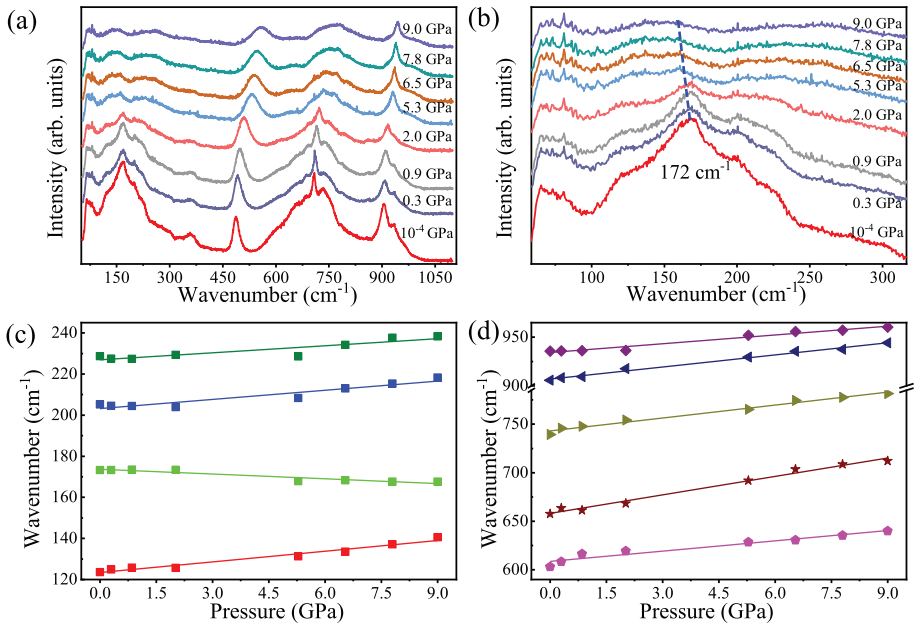

Fig. 3. (a, b) Raman spectra at different pressure and (c, d) pressure dependence of Raman modes of $Cs_2W_3O_{10}$. The solid lines are linear fitting to data of Raman modes at different pressure.

in Fig. 3a. It can be seen that the peak at 172 cm^{-1} gradually shifts to low wavenumber as changing pressure from atmospheric pressure to 9.00 GPa. In order to analyze the relationship between each vibration mode and pressure, Raman peaks were fitted by Lorentz peak profiles. The pressure-dependent shift of each mode is displayed in Fig. 3c and d. The frequencies of all observed modes exhibit linear dependence on pressure. The slopes $d\omega_i/dP$ listed in Table S2 have been obtained from each ω-P curve. It can be seen that the $d\omega_i/dP$ of mode at 172 cm^{-1} is negative, while others are positive. The mode Grüneisen parameters can be described as $\gamma_{iT} = \frac{B_T}{\omega_i}\left(\frac{d\omega_i}{dP}\right)_T$, in which B_T is the bulk modulus. It is clear that the mode with negative $d\omega_i/dP$ possesses negative Grüneisen parameter, which will contribute to NTE. Based on this, the mode at 172 cm^{-1} for W-O-W bending should be responsible for the abnormal thermal expansion of $Cs_2W_3O_{10}$.

According to the results above, the vibrations of two WO_6 octahedra libration modes and one W-O-W bending mode are possibly the origin of ZTE in $Cs_2W_3O_{10}$. Here, it should be noted that the W-O bond displays a covalent bond characteristic, while the nature of Cs-O bond has stronger ionic bonding property according to the results of first-principles calculation (Fig. S1 in Supporting information). The role of Cs is similar with the guests in NTE framework compounds such as $Na_xGaFe(CN)_6$ [49] and $AlPO_4$–17@O_2 [50]. So, it is important to further investigate the influence of WO_6 octahedra framework on the thermal expansion,

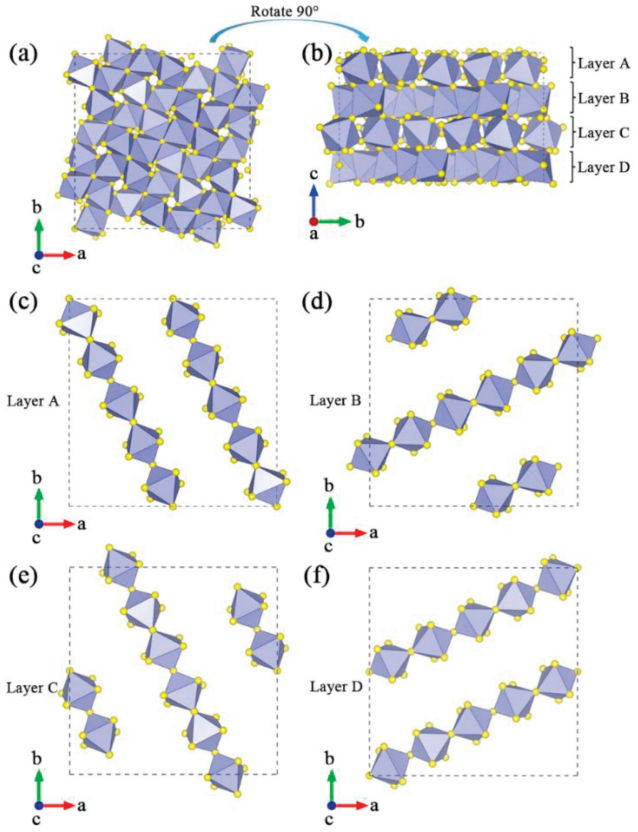

Fig. 4. Schematic diagram of projections in (a) *ab*- and (b) *bc*-plane and layers (c) A, (d) B, (e) C and (f) D in the *c*-axis direction for WO_6 octahedra framework.

the schematic of WO_6 octahedra framework obtained by omitting Cs atoms of the inset of Fig. 1a has been projected in *ab*- and *bc*-planes as displayed in Figs. 4a and b, respectively. In Fig. 4b, it can be seen that there are four layers of WO_6 octahedra arranged along *c*-axis direction in *bc*-plane. Each layer can be projected in *ab*-plane (Figs. 4c-f). The chains formed by WO_6 octahedra appear in each layer. In *ab*-plane, these chains are paved along different direction in different layer. It is clear that the *ab*-plane is composed of WO_6-octahedra-chains in the crystal structure of $Cs_2W_3O_{10}$. The vibrations of WO_6 octahedra libration should be related to these chains, which is possibly the origin of very low α_a. As for the vibration of W-O-W bending, it should be related to the transverse vibration of apical and equatorial oxygen atoms of WO_6 octahedra throughout the lattice. The further studies are still needed to clarify the vibration directions and the weighting of the two WO_6 octahedra libration modes and one W-O-W bending mode to the overall thermal expansion, which can help to understand the thermal expansion mechanism in framework material $Cs_2W_3O_{10}$.

The tetragonal tungstate $Cs_2W_3O_{10}$ has been synthesized by the solid state reaction method. The structure phase transition was not observed in the temperature-dependent XRD patterns and Raman spectra during the temperature measurement ranges. The cell parameters changed little as increasing temperature from 150 K to 573 K. The very low CTE of axes and volume indicated that the ZTE appeared in $Cs_2W_3O_{10}$. The temperature- and pressure-dependent Raman spectra showed that two WO_6 octahedra libration modes and one W-O-W bending mode should be responsible for the ZTE of $Cs_2W_3O_{10}$. This work provides one novel ZTE material of $Cs_2W_3O_{10}$, which gives insights into design new more ZTE materials with open-framework.

Declaration of competing interest

The authors declare that they have no known competing financial interests or personal relationships that could have appeared to influence the work reported in this paper.

Acknowledgments

This work was supported by the National Natural Science Foundation of China (Nos. 22071221, 21905252), and Natural Science Foundation of Henan Province (Nos. 212300410086, 222301420040 and 222300420325).

Supplementary materials

Supplementary material associated with this article can be found, in the online version, at doi:10.1016/j.cclet.2023.108957.

References

[1] B.H. Jin, J. Jang, D.J. Kang, et al., Compos. Sci. Technol. 224 (2022) 109456.
[2] K. Liu, F. Lu, X.S. Jia, et al., J. Mater. Chem. A 10 (2022) 24410–24421.
[3] J.S. Hu, F.K. Guo, M.C. Guo, et al., J. Mater. 6 (2020) 729–735.
[4] E.J. Liang, Q. Sun, H.L. Yuan, et al., Front. Phys. 16 (2021) 53302.
[5] K. Takenaka, Sci. Technol. Adv. Mater. 13 (2012) 013001.
[6] Q.L. Gao, S. Zhang, Y.X. Jiao, et al., Nano Res. 16 (2023) 5964–5972.
[7] Q. Li, K. Lin, Z. Liu, et al., Chem. Rev. 9 (2022) 8438–8486.
[8] L. Xie, F. Shi, C. Lin, et al., J. Mater. Sci. Technol. 146 (2023) 80–85.
[9] H.F. Liu, W.K. Sun, Z.P. Zhang, et al., Solids 2 (2021) 87–107.
[10] S. Xu, Y.M. Hu, Y. Liang, et al., Chin. Phys. B 29 (2020) 086501.
[11] Z.J. Ma, Y. Sun, H.Q. Lu, et al., Phys. Rev. B 107 (2023) 094412.
[12] Q.L. Gao, Y.X. Jiao, A. Sanson, et al., Chin. Chem. Lett. 34 (2023) 107564.
[13] G.H. Wu, C. Zhou, Q. Zhang, et al., Scr. Mater. 96 (2015) 29–32.
[14] S. Li, P. Kwon, Mater. Sci. Eng. A 527 (2009) 93–97.
[15] N. Xiao, Y.Q. Qiao, N.K. Shi, et al., Sci. China Technol. Sci. 64 (2021) 2057–2065.
[16] X.W. Shi, S. Zhang, Q. Zhou, et al., Tungsten 5 (2023) 179–188.
[17] T.E. Sarah, C. Felicity, F. Ian, et al., J. Am. Chem. Soc. 135 (2013) 12849–12856.
[18] Y. Zheng, Y.X. Jiao, Y.Q. Qiao, et al., Inorg. Chem. 62 (2023) 8543–8550.
[19] J.W. Xu, Z. Wang, H. Huang, et al., Adv. Mater. 35 (2023) 2208635.
[20] Q.L. Gao, Y.X. Jiao, Y. Zheng, et al., Results Phys. 36 (2022) 105410.
[21] Z.H. Ren, R.Y. Zhao, X. Chen, et al., Nat. Commun. 9 (2018) 1638.
[22] Q.L. Gao, X.W. Shi, A. Venier, et al., Inorg. Chem. 59 (2020) 14852–14855.
[23] Y. Li, Q.L. Gao, D.H. Chang, et al., J. Phys. Condens. Matter 32 (2020) 455703.
[24] Y.X. Gao, C.Y. Wang, Q.L. Gao, et al., Inorg. Chem. 59 (2020) 18427–18431.
[25] X.X. Jiang, M.S. Molokeev, P.F. Gong, Adv. Mater. 36 (2016) 7936–7940.
[26] C.P. Romao, F.A. Perras, U. Werner-Zwanziger, et al., Chem. Mater. 27 (2015) 2633–2646.
[27] Q.L. Gao, J.Q. Wang, A. Sanson, et al., J. Am. Chem. Soc. 142 (2020) 6935–6939.
[28] Q.L. Gao, Q. Sun, A. Venier, et al., Sci. China Mater. 65 (2022) 553–557.
[29] S.F. Solodovnikov, O.A. Mankova, Z.A. Solodovnikova, et al., J. Struct. Chem. 37 (1996) 645–650.
[30] M. Zhang, Z.P. Lian, Y. Wang, et al., RSC Adv. 6 (2016) 339234–339239.
[31] Y.Q. Zhao, F.Y. Han, Q. Wang, et al., ChemCatChem 8 (2016) 624–630.
[32] N. Tahmasbi, S. Madmoli, P. Farahnak, et al., Russ. J. Appl. Chem. 90 (2017) 1488–1493.
[33] A.E. Phillips, A. Dominic Fortes, Angew. Chem. Int. Ed. 56 (2017) 15950–15953.
[34] Y. Iwai, M. Nakaya, H. Ohtsu, et al., CrystEngComm 24 (2022) 5880–5884.
[35] Q.L. Gao, Y.X. Jiao, G. Li, Chin. Phys. B 31 (2022) 046501.
[36] A. Sleight, Nature 425 (2003) 674–676.
[37] K. Takenaka, H. Takagi, Appl. Phys. Lett. 94 (2009) 131904.
[38] Y.G. Du, Q.L. Gao, A. Sanson, et al., Results Phys. 35 (2022) 105415.
[39] M. Boulova, N. Rosman, P. Bouvier, et al., J. Phys. Condens. Matter 14 (2002) 5849–5863.
[40] M. Maczka, A.G. Souza, P.T.C. Freire, et al., J. Raman Spectrosc. 34 (2003) 199–204.
[41] A. Basu, S. Paul, M. Polentarutti, et al., J. Phys. Condens. Matter 23 (2011) 365401.
[42] L. Aleksandrov, T. Komatsu, R. Iordanova, et al., Opt. Mater. 34 (2011) 201–206.
[43] M. Maczka, L. Macalik, K. Hermanowicz, et al., J. Raman Spectrosc. 41 (2010) 1059–1066.
[44] K.P. da Silva, W. Paraguassu, M. Maczka, et al., J. Raman Spectrosc. 42 (2011) 474–481.
[45] H.L. Yuan, Q.L. Gao, P. Xu, et al., Inorg. Chem. 60 (2021) 1499–1505.
[46] H.L. Yuan, C.Y. Wang, Q.L. Gao, et al., Inorg. Chem. 59 (2020) 4090–4095.
[47] R. Mittal, M. Zbiri, H. Schober, et al., Phys. Rev. B 83 (2011) 024301.
[48] T. Basak, M. Rao, S.L. Chaplot, et al., Phys. B 433 (2014) 149–156.
[49] Q.L. Gao, N.K. Shi, A. Sanson, et al., Inorg. Chem. 57 (2018) 14027–14030.
[50] F. Alabarse, B. Baptiste, B. Joseph, et al., J. Phys. Chem. Lett. 13 (2022) 9390–9395.